fishes

IMPACT FACTOR 2.9

CITESCORE 4.4

Review

From Gills to Tissues: An Oxygen-Cascade Perspective on Metabolic Scaling in Fishes

Cosmas I. Nathanailides

Special Issue

Feature Papers by *Fishes*' Editorial Board Members

Edited by

Prof. Dr. Maria Angeles Esteban

MDPI

https://doi.org/10.3390/fishes11080439

fishes

MDPI

Review

From Gills to Tissues: An Oxygen-Cascade Perspective on Metabolic Scaling in Fishes

Cosmas I. Nathanailides

Department Agriculture, University of Ioannina, GR 47100 Arta, Greece; nathan@uoi.gr

Abstract

Data of experimental, comparative, and allometric studies was examined in relation to the wider oxygen transport cascade, including branchial ventilation, diffusion across the water–blood barrier, blood oxygen transport, muscle capillarization, and mitochondrial content. Experimental reductions in functional gill area are associated with lower maximal oxygen consumption and reduced critical swimming speed, whereas reversible gill remodelling may increase exposed lamellar surface under hypoxia or increased oxygen demand. Comparative evidence indicates that gill area accounts for a measurable, but incomplete, component of variation in metabolic rate and hypoxia tolerance. A descriptive comparison of ten published paired gill surface area (GSA) and standard metabolic rate (SMR) datasets did not reveal a consistently negative difference between gill surface area and standard metabolic demand across the species and experimental conditions examined. This comparison addresses maintenance metabolism but does not test oxygen-supply constraints during routine or maximal activity. The broader evidence reviewed includes large salmonids with cardiovascular compensation, cyprinids with reversible gill remodelling, haemoglobinless icefishes, and active pelagic taxa with high cardiorespiratory and locomotor investment. Collectively, these examples show that the functional significance of gill area depends on interacting branchial, cardiovascular, haematological, tissue-level, and ecological traits.

Keywords: fish metabolism; mitochondria; oxygen transport; climate change

Key Contribution: This review suggests that the capacity for aerobic metabolism of fishes is best understood through an integrated oxygen-cascade framework rather than by gill surface area alone which becomes predictive only under certain physiological and ecological conditions.

Academic Editor: Maria Angeles Esteban

Received: 27 June 2026
Revised: 20 July 2026
Accepted: 24 July 2026
Published: 26 July 2026

1. Introduction

Gill-centred hypotheses, most notably the Gill-Oxygen Limitation Theory (GOLT), have been influential in linking respiratory surface area with fish growth, maximum body size, maturation, and sensitivity to warming [1,2]. In its strong form, GOLT predicts that branchial surface area scales less steeply than oxygen demand as body size increases, producing a progressive mismatch between oxygen uptake capacity and metabolic requirement that may constrain growth, maximum body size, and responses to warming. Under global warming scenarios, the thermal elevation of metabolic oxygen demand coincides with reduced oxygen solubility and altered diffusion kinetics in water, narrowing the functional margin between oxygen supply and demand. The present synthesis draws on this context but departs from treatments of gill surface area as a singular determinant of aerobic performance. The central question is not whether branchial respiratory surface

matters, but rather under what physiological conditions its predictive value is realised and when it is not. The comparison below addresses a more circumscribed version of this question, as follows: whether published intraspecific standard metabolic rate (SMR) datasets contain evidence of a size-dependent mismatch between gill surface area and baseline metabolic oxygen demand. SMR represents the minimum oxygen uptake required to support essential maintenance functions in a post-absorptive, inactive, and thermally acclimated fish [3].

Gill respiratory surface represents the anatomical boundary through which oxygen enters the organism from water, yet its functional contribution to aerobic capacity cannot be assessed in isolation. Oxygen flux through the cascade depends equally on branchial ventilation, diffusion across the water–blood barrier, haemoglobin-mediated transport, cardiac output, capillary exchange at the level of skeletal muscle, and terminal mitochondrial oxygen consumption [4–6]. Experimentally, partial reductions in functional gill area have been associated with decreased maximal oxygen uptake and impaired critical swimming speed, whereas exposure to hypoxia or sustained exercise can promote lamellar remodelling that increases the exposed respiratory surface [7–9]. Comparative data, by contrast, indicate that gill area accounts for only a portion of interspecific variation in metabolic rate and hypoxia tolerance [10–12], a pattern that implies constraint by downstream components of the transport pathway.

The present study examines the degree to which gill surface area accounts for interspecific variation in aerobic capacity, hypoxia tolerance, and thermal sensitivity in fishes, and investigates how this relationship is modified by downstream components of oxygen transport and oxygen use. Particular attention is given to blood oxygen-carrying capacity, cardiac delivery, muscle capillarity, mitochondrial phenotype, body size, ventilatory capacity, and ecological strategy, traits that collectively determine whether the oxygen entering at the branchial surface can be delivered and utilised at a rate commensurate with metabolic demand. It is suggested that gill surface area is best interpreted as a conditional rather than an absolute predictor of aerobic capacity, one whose explanatory power depends on the functional state of the downstream transport pathway rather than on its anatomical dimensions alone.

This review integrates experimental studies of gill form and function, comparative analyses linking gill surface area with metabolic rate, hypoxia tolerance, or swimming performance, and studies of blood, cardiac, and muscular traits that modify oxygen transport downstream of branchial uptake. The allometric comparison is restricted to published SMR scaling exponents and is used to examine whether available baseline metabolic datasets support a size-dependent mismatch between gill surface area and standard metabolic demand. This review aims to evaluate gill surface area within the wider oxygen-transport cascade that supports aerobic performance under different physiological and environmental conditions. A second aim is a comparison of some examples of published GSA and SMR scaling exponents to address a narrower question of whether there is a consistent size-related decline in gill surface area relative to maintenance oxygen demand. The latter is not used as a test of oxygen-supply limitation during routine swimming or maximal activity.

2. Form and Function of Gill Respiratory Surface

The gill respiratory surface represents the principal morphological interface for oxygen transfer from water to blood. Its functional importance is most evident when the exposed exchange area is experimentally, environmentally, or pathologically altered. In rainbow trout, a reduction in functional gill area of approximately 27–30% reduced maximum oxygen consumption by about 27–29% and significantly impaired critical swimming speed [7]. In Atlantic salmon, amoebic gill disease reduced aerobic scope and swimming perfor-

mance [9]. In goldfish, acclimation to hypoxia or sustained exercise increased exposed lamellar surface area and improved swimming performance under hypoxia [8], while exercise-remodelling experiments further demonstrated that changes in the interlamellar cell mass can influence aerobic swimming capacity [13].

Functional respiratory surface area is not equivalent to total anatomical gill size. Diffusion distance across the water–blood barrier, lamellar perfusion, ventilatory flow, and the presence of an interlamellar cell mass can all modify effective oxygen-transfer capacity. In goldfish and crucian carp, normoxia at low temperatures promotes development of the interlamellar cell mass and reduces exposed lamellar surface area, whereas hypoxia or warming induces its regression and increases the surface of the lamellae exposed to water [14–17]. This reversible remodelling demonstrates that gill area should be interpreted as a functional and plastic trait rather than as a fixed anatomical constant.

Anatomical gill surface area should also be distinguished from realised branchial oxygen-transfer capacity, which depends not only on the dimensions of the exchange surface but also on water flow across the lamellae and blood flow through the lamellar capillaries. Ventilation frequency and ventilatory stroke volume can therefore modify oxygen transfer without any corresponding change in total anatomical gill area. Across six closely related cyprinid species, the scaling of resting metabolic rate was related jointly to the scaling of both gill surface area and ventilation frequency, indicating that metabolic scaling cannot be attributed to exchange area alone [18]. This interaction was demonstrated experimentally in goldfish, as follows: surgical removal of approximately half of the gill surface reduced oxygen uptake per ventilatory cycle by about 60% but did not alter resting metabolic rate or its body-mass scaling exponent. Instead, ventilation frequency increased from 21.6 to 52.8 ventilatory movements min^{-1}, apparently compensating for the reduced exchange surface [19].

Consistent with this functional interpretation, comparative evidence supports an important contribution of gill area to aerobic capacity while also delineating its explanatory limits. Gill surface area explained approximately 27% of the interspecific variation in oxygen consumption after accounting for body mass [11]. Gill morphology also contributes to variation in hypoxia tolerance. In sculpins, greater hypoxia tolerance was associated with larger mass-specific gill surface area, lower routine oxygen demand, and higher haemoglobin-oxygen affinity [5]. Likewise, in centrarchid sunfishes, gill area was related to hypoxia tolerance and exercise capacity, whereas axial-muscle capillarity was more specifically associated with aerobic swimming performance [10].

3. Components of Fish Oxygen Transport Cascade

3.1. Blood and Heart

The blood and heart link branchial uptake to tissue oxygen delivery. A fish with large gills may still be limited if haemoglobin concentration, oxygen affinity, cardiac output, or peripheral perfusion cannot sustain the necessary flux. Conversely, cardiovascular compensation may reduce the functional impact of declining mass-specific gill area during growth.

Comparative and experimental studies illustrate this point. In sculpins, low critical oxygen tension was not explained by gill area alone, but by a combination of larger mass-specific gill surface area, lower routine oxygen demand, and higher haemoglobin oxygen affinity [5]. In Chinook salmon, Clark and Farrell [6] reported that heart rate and acceleration activity did not follow a universal negative body-mass scaling relationship in mature fish; compact myocardium, ventricular mass, and spleen mass scaled nearly isometrically. In rainbow trout, cardiac oxidative traits increased with body size, suggesting that cardiac metabolic capacity may be remodelled during growth [20]. In growth hormone transgenic Atlantic salmon, enhanced cardiac output, haemoglobin concentration, and muscle oxida-

tive enzyme activities did not prevent lower metabolic scope and reduced critical swimming speed because gill surface area was not similarly enhanced, suggesting a branchial oxygen-transfer constraint despite downstream cardiovascular compensation [21].

Direct measurements of pO2 in rainbow trout provide strong support for this interpretation. Kuchenmuller et al. [22] examined arterial and venous oxygen partial pressures across a wide body-mass range during acute warming, hyperoxia, and exhaustive exercise. Arterial pO2 did not show significant negative scaling with body mass during resting warming, suggesting no clear size-dependent limitation of gill oxygen uptake under resting conditions. By contrast, venous pO2 declined significantly with body mass at both 18 degrees C and 25 degrees C, indicating reduced cardiac oxygen availability in larger fish. After exhaustive exercise at 25 degrees C, arterial pO2 also declined with body mass, suggesting that branchial oxygen uptake may become limiting only when thermal and physical stress are combined.

Myocardial capillarization may also adjust to cardiac workload, although anatomical capillary density should not be interpreted as a direct measure of whole-animal aerobic capacity. In seasonally acclimatized rainbow trout, ventricular capillary density was highest at 18 degrees C and broadly paralleled heart rate, consistent with greater local myocardial workload at warmer temperatures. However, cardiac output was depressed at the warm temperature despite the high capillary density, indicating that myocardial capillary supply was not the principal functional limitation under these conditions [23]. In contrast, capillary length density in slow locomotory muscle was maximal at 11 degrees C, coinciding with the highest muscle blood flow and greatest aerobic swimming scope. These contrasting responses show that capillarisation is tissue-specific and that its functional significance depends on perfusion, vascular topology, tissue geometry, and oxidative demand rather than on capillary density alone [24].

These findings place cardiac oxygen supply, rather than gill area alone, as a key size-dependent issue for aerobic capacity of large fish. Large salmonids may not conform to simple oxygen limitation predictions because cardiac and haematological traits can preserve or enhance oxygen delivery. Icefishes provide an even more extreme case, as follows: the absence of haemoglobin shifts oxygen transport toward high blood volume, enlarged hearts, high cardiac output, and tissue-level diffusion adaptations [25,26]. Such taxa illustrate why gill surface area must be considered together with the capacity of the circulatory system to move oxygen from the branchial surface to the tissues.

3.2. Tissue Oxygen Delivery and Mitochondrial Phenotype

The terminal oxygen-use stage of the oxygen cascade encompasses all metabolically active tissues. Oxygen delivered through the branchial and cardiovascular systems ultimately supports mitochondrial ATP production in organs with continuous maintenance demands, including the myocardium, gill epithelium, and visceral tissues. In many fishes, however, aerobic capacity must support not only maintenance metabolism but also the prolonged, submaximal swimming required for routine activities such as station holding, foraging, and migration. Gatz [27] emphasised the distinct locomotor functions of fish muscle fibres, identifying red muscle as the principal tissue supporting stamina and sustained swimming, in contrast to the recruitment of white muscle during brief, high-speed activity.

Importantly, the contribution of a tissue to whole-animal aerobic metabolism depends not only on its mass but also on its metabolic intensity and mitochondrial phenotype. In brown trout, Norin and Malte [28] found that variation in the mass of the liver, heart, spleen, intestine, and stomach did not explain individual differences in standard metabolic rate, maximum metabolic rate, or aerobic scope. By contrast, tissue-specific cytochrome-c oxidase activity was positively related to both standard and maximum metabolic rate. Nev-

ertheless, the relative contribution of different tissues to whole-animal oxygen consumption changes with physiological state. During digestion, for example, oxygen demand and blood flow increase substantially in gastrointestinal and assimilatory tissues. In rainbow trout, Eliason et al. [29] reported that peak postprandial oxygen consumption increased from 48.4 to 94.6 mg O_2 kg^{-1} h^{-1}, corresponding to an approximately 1.95-fold elevation above standard metabolic rate. Gastrointestinal blood flow increased concurrently from 4.2 to 9.9 mL min^{-1} kg^{-1}, representing an approximately 2.36-fold increase.

Changes in whole-animal metabolic rate reflect not only the capacity of the oxygen-supply pathway but also the metabolic demand generated by maintenance, digestion, growth, reproduction, and locomotion. An integrated analysis of an aquatic crustacean showed that the ontogenetic scaling of metabolism may be associated with the scaling of food assimilation, somatic growth, and reproductive investment, and therefore need not be interpreted solely as a passive consequence of resource-supply constraints [30].

During sustained swimming, Richards et al. [31] found that whole-animal oxygen consumption increased 1.5-fold at 30% Ucrit and 2.2-fold at 60% Ucrit. This increase was accompanied by pronounced activation of red-muscle oxidative metabolism, as follows: during the first 2 min of swimming, pyruvate dehydrogenase activity increased 4-, 8-, and 12-fold at 30%, 60%, and 90% Ucrit, respectively. At 90% Ucrit, red-muscle pyruvate dehydrogenase activity remained approximately 10- to 12-fold above control values during the swimming period.

The myocardium also operates continuously and requires a sustained aerobic energy supply, while mitochondria-rich ionocytes of the gill epithelium support the substantial ATP requirements of active ion transport, principally through Na+/K+-ATPase-dependent processes involved in osmoregulation and acid-base regulation [4,32]. Thus, SMR reflects oxygen use across multiple organs and tissues, whereas the specific emphasis on red muscle becomes most relevant when the cascade is evaluated in relation to routine and sustained swimming performance.

Changes in the capillarization of skeletal muscle tissue can indicate changes associated with the final delivery path from blood to muscle fibers. In sunfishes, axial muscle capillarity was more closely associated with aerobic swimming performance than gill area alone, even though gill area contributed to hypoxia tolerance and exercise capacity [10]. Gill respiratory surface may therefore define the potential for oxygen uptake, whereas capillary supply, fibre diameter, and intracellular diffusion distance determine how efficiently that oxygen reaches mitochondria in active muscle.

Mitochondrial phenotype represents the terminal oxygen-use step, but it should not be inferred from mitochondrial volume density alone. Low-temperature responses of fish muscle can involve changes in mitochondrial abundance, cristae density, oxidative enzyme activities, and substrate use, but the direction and magnitude of these responses vary with species, tissue, activity pattern, and thermal history [33]. Oxidative enzyme activities, including cytochrome c oxidase and citrate synthase, provide functional indices of aerobic capacity that may vary with growth and temperature [34,35]. In Atlantic salmon, cytochrome c oxidase and lactate dehydrogenase activities differed between slow- and fast-growing groups, indicating variation in the balance between oxidative and glycolytic ATP production [36]. Seasonal work on red porgy similarly showed coordinated changes in metabolic gene expression and enzyme activities, including LDH, citrate synthase, cytochrome c oxidase, and HOAD, suggesting that thermal acclimatization can reorganize tissue substrate use and oxidative capacity [37]. In carp, acclimation to summer and winter temperatures altered muscle capillarization, oxygen diffusion distances, and mitochondrial content [38]. In striped bass, relative mitochondrial volume density declined from about 40% of fibre volume in smaller individuals to about 30% in larger individuals, while total

mitochondrial content per fibre increased as fibres enlarged [39]. Thermal acclimation can also modify mitochondrial structure and function, as follows: cold-acclimated striped bass showed increased mitochondrial volume density in slow fibres [40], whereas rainbow trout increased cristae surface density and oxidative capacity without necessarily increasing mitochondrial volume density [41].

The link between gill area and thermal sensitivity should therefore be interpreted through the whole oxygen cascade and in light of the continuing debate around aerobic scope and oxygen- and capacity-limited thermal tolerance. Warm-temperature-induced reductions in body size, and the temperature-size rule more generally, are best treated as integrated ontogenetic responses in which oxygen supply, metabolic demand, development rate, and ecological context interact rather than as direct consequences of gill area alone [42]. Body mass and cell size have been shown to shape low-oxygen tolerance in fishes in a temperature-dependent manner [43]. Elevated temperature and hypoxia do not act as independent stressors; their interaction may determine whether aerobic performance is maintained, with plasticity in ventilation, branchial remodelling, circulatory adjustments, and mitochondrial function all potentially contributing to the outcome [44,45]. Aerobic scope retains utility as a functional index of oxygen-demanding capacity, though its thermal optimum and ecological interpretation are not fixed quantities; both vary with experimental protocol, activity state, life stage, and the ecology of the species under investigation [46–48].

In red porgy, warm seasonal acclimatization was associated with reduced cardiac COX1 activity and lower energy consumption, suggesting that cardiac metabolism may become constrained during seasonal warming [37]. In the present synthesis, aerobic scope is therefore treated as one functional expression of the integrated oxygen transport cascade, rather than as a direct consequence of gill area alone.

3.3. Body Form Skeletal Muscle and Swimming Metabolism

Body form and swimming ecology influence oxygen demand and therefore determine how strongly gill area should predict performance. Active pelagic fishes generally experience sustained locomotor demands and are expected to show high investment in branchial, cardiovascular, and muscular oxygen transport. Benthic or intermittently active species may rely on different combinations of hypoxia tolerance, low routine oxygen demand, ventilatory plasticity, or anaerobic capacity. These ecological contrasts are important because the final steps of the oxygen cascade are modified by muscle capillarity, fibre geometry, and mitochondrial phenotype, as follows: axial muscle capillarity is associated with aerobic swimming performance in sunfishes [10], fibre growth can alter intracellular diffusion geometry during ontogeny [39], mitochondrial structure and oxidative capacity can be remodelled by thermal acclimatisation [41], and exceptional mitochondrial phenotypes may contribute to oxygen diffusion in haemoglobinless Antarctic fishes [23]. Morphological traits such as body depth, fineness ratio, caudal fin aspect ratio, relative red muscle mass, and head/body proportions can therefore provide ecological context for interpreting gill area (Table 1).

In addition to the evidence presented in Table 1, there are several examples of comparative evidence which are also consistent with this oxygen cascade approach of gills (Table 2). Bluefin tuna and European horse mackerel show positive bS values in the Scheuffele et al. [12] dataset, indicating that gill surface area scales more steeply than standard metabolic demand across the available size ranges. High positive bS values which indicate a relatively high investment in respiratory surface area are exhibited in active pelagic taxa, where sustained locomotor demand places a premium on branchial oxygen uptake capacity. Cyprinids such as goldfish, carp, and tench present a contrasting pattern, combining

comparatively low routine oxygen demand with considerable branchial plasticity and hypoxia tolerance.

Table 1. Downstream muscle traits that modulate the functional significance of changes in gill area into aerobic capacity of skeletal muscle.

Trait	Functional Role in the O_2 Cascade	Representative Evidence	Interpretation
Muscle capillarity	Controls the final blood-to-fibre diffusion pathway.	Axial muscle capillarization is strongly associated with aerobic swimming performance [1].	Gill area may support oxygen uptake, but capillarity influences whether oxygen reaches active muscle efficiently.
Fibre diameter and diffusion distance	Determine intracellular path length for O_2 movement.	Structural remodelling of muscle fibres during growth [39].	Large fibres can increase diffusion distance unless compensated by capillarity or mitochondrial distribution.
Mitochondrial volume density	Represents the volume fraction of muscle fibre occupied by mitochondria.	Striped bass show a decline from about 40% to 30% during growth, while total mitochondrial content per fibre increases [39].	Relative density does not necessarily rise with growth; absolute mitochondrial content and fibre architecture matter.
Cristae surface density and enzyme capacity	Reflect mitochondrial quality and oxidative membrane surface.	Cold acclimation induced an increase in cristae surface density without a significant increase in mitochondrial volume density [41].	Mitochondrial function cannot be inferred from volume density alone.
Exceptional mitochondrial phenotypes	May facilitate diffusion as well as ATP production.	Antarctic icefishes have high mitochondrial volume density in oxidative muscle [25].	High mitochondrial density may compensate for unusual blood oxygen transport constraints.

Table 2. Standard metabolic-rate (SMR) examples which link gill respiratory surface and metabolic demand. Data from Scheuffele, Jutfelt and Clark [12].

Fish Species	b_{GSA} (SE)	b_{SMR} (SE)	$b_S = b_{GSA} - b_{SMR}$ (SE; 95% CI)	Interpretation
European eel (*Anguilla anguilla*)	0.90 (0.10)	0.83 (0.09)	0.07 (0.14; −0.19 to 0.34)	Near-zero difference; no clear decline in GSA relative to SMR.
Common carp (*Cyprinus carpio*)	0.83 (0.04)	0.80 (0.06)	0.03 (0.07; −0.11 to 0.16)	Near-parallel scaling of gill area and standard metabolism.
European flounder (*Platichthys flesus*)	0.70 (0.04)	0.77 (0.17)	−0.08 (0.17; −0.42 to 0.26)	Slightly negative but uncertain because the confidence interval includes zero.
Atlantic salmon (*Salmo salar*)	0.97 (0.02)	1.07 (0.02)	−0.09 (0.03; −0.16 to −0.03)	GSA scales more slowly than SMR across the available size range.
Marbled electric ray fish (*Torpedo marmorata*)	0.65 (0.18)	0.97 (0.24)	−0.32 (0.30; −0.92 to 0.27)	Negative estimate, but uncertainty is large.
Goldfish (*Carassius auratus*), 15 °C	0.74 (0.06)	0.87 (0.07)	−0.13 (0.09; −0.31 to 0.05)	Possible decline in GSA relative to SMR under this acclimation condition.
Goldfish (*Carassius auratus*), 25 °C	0.87 (0.04)	0.83 (0.04)	0.04 (0.05; −0.07 to 0.15)	Near-parallel scaling under warmer acclimation.
European horse mackerel (*Trachurus trachurus*)	1.23 (0.03)	0.89 (0.08)	0.34 (0.08; 0.17 to 0.50)	GSA scales more steeply than SMR.
Tuna (*Thunnus* spp.)	0.99 (0.09)	0.71 (0.03)	0.28 (0.09; 0.11 to 0.46)	Positive difference; consistent with high respiratory investment in an active pelagic taxon.
Nile tilapia (*Oreochromis niloticus*)	0.67 (0.05)	0.64 (0.02)	0.025 (0.05; −0.08 to 0.13)	Near-zero difference; GSA and SMR scale similarly.
Descriptive arithmetic means across the ten SMR datasets (Calculated from Scheuffele et al., [12])	0.855	0.838	0.0165	Descriptive arithmetic mean is close to zero; individual comparisons vary in direction and magnitude.
Secondary inverse-variance-weighted descriptive summary			0.0004 (95% CI −0.038 to 0.039)	Weighted mean close to zero.

Note. Only standard metabolic rate (SMR) datasets are included in this table. Active metabolic rate datasets reported by Scheuffele, Jutfelt and Clark [12] were excluded from the SMR summary because they represent elevated metabolic demand rather than baseline maintenance metabolism.

3.4. Analytical Scope and Limitations of the Descriptive Allometric Comparison

The comparison presented below is a structured descriptive reanalysis of published paired scaling exponents rather than a formal meta-analysis. It addresses a narrow question, as follows: whether the available intraspecific datasets show a consistent decline in gill surface area relative to standard metabolic demand across the body-size ranges examined. The numerical comparison was restricted to the ten datasets compiled by Scheuffele et al. [12] for which directly comparable scaling exponents and standard errors for gill surface area (GSA) and standard metabolic rate (SMR) were available.

This restriction provided a common analytical basis across the comparisons, as follows: each dataset reported paired GSA and SMR exponents, represented the same baseline metabolic state, and included the uncertainty required to calculate the standard error and approximate confidence interval of $b_{GSA} - b_{SMR}$.

The number of comparisons reflects the limited availability of published studies meeting these comparability criteria rather than selective inclusion according to the direction of the results. Each entry represents a published slope estimate derived from multiple individuals across a reported body-size range. Nevertheless, these ten datasets are used only to determine whether this available comparable evidence exhibits a uniform directional pattern.

Additional studies have examined ontogenetic relationships among respiratory surface area, body mass, and metabolic demand in fishes, including carp, larval and juvenile walleye, Japanese flounder, and the California horn shark [49–52]. These studies were incorporated into the broader physiological interpretation but were not added to the paired numerical comparison when they differed in the respiratory surface measured, metabolic endpoint, developmental interval, or form of the reported relationship, or when the uncertainty required for calculating a paired difference was unavailable. Forcing such studies into a single quantitative summary would obscure biologically important ontogenetic transitions and reduce methodological comparability.

In larval and juvenile walleye, the relative contributions of cutaneous and branchial respiratory surfaces changed markedly during development, with skin dominating the available exchange area immediately after hatching and branchial area becoming progressively more important as the fish grew [50]. This developmental transition cautions against applying a single branchial-surface exponent across early ontogeny. Likewise, during early development of Japanese flounder, resting-metabolism scaling corresponded more closely to body-surface scaling than to respiratory-area scaling [51]. Ontogenetic phase shifts in metabolic scaling have also been documented in sterlet sturgeon, indicating that stage-dependent scaling is not restricted to teleost fishes [53].

In the present study, for each dataset, the difference between the GSA and SMR scaling exponents was calculated as follows: $b_S = b_{GSA} - b_{smr}$.

Positive values of bs indicate that GSA scaled more steeply than SMR, negative values indicate that SMR scaled more steeply than GSA, and values close to zero indicate approximately parallel scaling. The standard error of each difference was approximated as follows:

$$SE_{b_S} = \sqrt{SE^2_{b_{GSA}} + SE^2_{b_{SMR}}}$$

The present analysis was based on the assumption of independence between the published slope estimates because covariance terms were unavailable. Approximate 95% confidence intervals were calculated as $b_S \pm 1.96 SE_{b_S}$.

Arithmetic and inverse-variance-weighted mean differences were also calculated as secondary descriptive summaries. However, the datasets differ in species, temperature, life stage, body-size range, and experimental conditions and were not identified through a

systematic meta-analytic sampling procedure. They are therefore not assumed to estimate a single common biological effect. The pooled values are reported only as sensitivity summaries, while the principal interpretation is based on the direction, magnitude, and consistency—or lack of consistency—of the individual paired differences.

The comparison also inherits the assumption that each published relationship can be represented adequately by a single log-linear scaling exponent across the reported body-size range. Ontogenetic changes in respiratory mode, body form, tissue composition, activity, and developmental stage may produce nonlinear relationships or phase shifts in both GSA and metabolic scaling. A single exponent may consequently average biologically distinct ontogenetic intervals and conceal size ranges over which a mismatch is present or absent.

There is some evidence which indicates that standard and maximum metabolic rates need not scale in parallel throughout ontogeny. Killen et al. [54] found that the scaling of both SMR and maximum metabolic rate (MMR) changed across developmental stages in marine teleosts, particularly around metamorphosis. Chabot et al. [3] similarly cautioned that the SMR scaling exponent may differ between larval and post-larval life stages. The comparisons should therefore be interpreted as specific to the life stages and body-size ranges represented in each source dataset rather than as fixed species-level scaling relationships [12,49,51,53–55].

Relevant paired evidence comes from the California horn shark, in which resting and maximum metabolic rate scaled with exponents of 0.966 and 1.073, respectively, while GSA showed an ontogenetic breakpoint, as follows: its exponent was relatively shallow in individuals below 0.203 kg but increased to approximately isometric scaling later in life [52]. In carp, the relationship between GSA and body mass was triphasic, with markedly different prelarval, postlarval, and juvenile–adult slopes. Most of these phase-specific GSA slopes did not correspond to the scaling of resting metabolism, demonstrating that a single exponent across the full ontogenetic range could obscure biologically distinct developmental relationships [49]. More broadly, age-specific metabolic scaling may reflect changing demands associated with growth, development, and activity, as well as changes in resource-supply capacity [52,55].

For most of the analysed ontogenetic range, GSA is scaled between resting and maximum metabolic demand. This illustrates that the relationship among GSA, resting demand, and maximum demand can change during ontogeny and cannot necessarily be represented by a single species-level exponent.

In the present study, the analysis is focused on SMR and does not test whether GSA constrains routine swimming metabolism, active or maximum metabolic rate, aerobic scope, growth, warming tolerance, hypoxia tolerance, or disease resistance. SMR represents the standardized baseline oxygen demand that the oxygen-transport cascade must continuously support, but it does not quantify the additional oxygen costs of routine or maximal activity. The aim is to examine whether the available datasets show a consistent size-dependent decline in GSA relative to maintenance metabolic demand. This approach offers a method to explore the oxygen-cascade framework which is central to the present study.

3.5. Comparison of Gill Surface Area and SMR Scaling

Across the ten paired SMR datasets, the difference between the gill surface area and SMR scaling exponents varied in magnitude among species and experimental conditions.

Some datasets showed negative differences, others showed values close to zero, and others showed positive differences. Thus, the available comparisons did not reveal a consistently negative relationship in which gill surface area scaled more slowly than standard metabolic demand. The arithmetic mean difference was close to zero, but this

value is used only as a descriptive summary because the datasets are heterogeneous and cannot be assumed to represent a common underlying effect. The principal result is therefore the absence of a uniform directional pattern rather than evidence for a universal average scaling relationship. More specifically, across the ten SMR datasets reported by Scheuffele et al. [12], the arithmetic mean gill surface area exponent was $b_{GSA} = 0.855$, and the arithmetic mean standard metabolic exponent was $b_{SMR} = 0.838$, giving a mean paired difference of $b_S = 0.0165$. As a secondary descriptive sensitivity summary, inverse-variance weighting produced a mean difference of 0.0004, with an approximate 95% confidence interval from −0.038 to 0.039. These values are reported for completeness but are not interpreted as estimates of a universal cross-species effect because the datasets differ in species, environmental conditions, and body-size ranges.

Several examples illustrate this divergence. Common carp, goldfish at 25 °C, and Nile tilapia show near-parallel scaling of gill area and standard metabolism. Atlantic salmon and goldfish at 15 °C show negative bS values, suggesting that standard metabolic demand increases more steeply than gill surface area over the available ranges. European horse mackerel and bluefin tuna show positive bS values, indicating higher relative respiratory investment with size.

The single AMR dataset available for Nile tilapia was not incorporated into the SMR summary because it represents a different metabolic state and cannot support a cross-species synthesis of elevated metabolic demand. It nevertheless illustrates that GSA–metabolism relationships may differ with activity state. Broader conclusions concerning routine or maximal aerobic demand require matched GSA, AMR/MMR and aerobic-scope datasets from multiple species.

Standard metabolic rate represents the minimum rate of oxygen uptake required to support essential maintenance functions in a post-absorptive, inactive, and thermally acclimated fish [3]. It therefore defines the standardised lower boundary of whole-animal aerobic metabolism, rather than a measure of routine swimming or maximal aerobic performance. SMR quantifies the continuous oxygen cost of maintaining ion gradients, circulation, ventilation, protein turnover, tissue integrity, and other essential physiological functions. These costs depend strongly on the relative mass and activity of metabolically expensive organs. Rosenfeld et al. [56] identified the digestive tract, liver, kidney, heart, and gills as tissues that may contribute disproportionately to whole-animal SMR and argued that ontogenetic changes in their relative mass and metabolic activity can contribute to SMR scaling. In rainbow trout, Allen et al. [57] further showed that a fast-growing strain had a higher SMR, a larger gastrointestinal tract, and a lower aerobic scope, demonstrating that baseline oxygen demand reflects integrated investment in growth-supporting tissues and directly influences the aerobic capacity remaining for other physiological functions. Because aerobic scope is defined as the difference between maximum and standard metabolic rate, the scaling of SMR determines how much of the total aerobic capacity is already committed to maintenance before the additional demands of locomotion, digestion, or environmental stress are imposed [56,57]. Broader conclusions concerning routine or maximal aerobic demand require matched GSA, AMR/MMR, and aerobic-scope datasets from multiple species.

Accordingly, the focus of the present study on the comparison of gill-surface-area and SMR scaling does not assume that gill area determines SMR, nor does it use SMR as a proxy for maximal aerobic performance. Rather, it addresses the narrower but biologically important question of whether the anatomical surface available for branchial oxygen uptake scales commensurately with the obligatory baseline oxygen demand that must be continuously supported as fish grow. Rosenfeld et al. [56] noted that standard metabolic demand is generally below the upper oxygen-delivery ceiling imposed by respiratory

structures; the present comparison should therefore be regarded as a conservative test of the lowest standardised demand placed on the oxygen-transport cascade. The absence of a consistent mismatch at the SMR level observed in the present study, does not exclude the possibility that a mismatch emerges as oxygen demand rises during routine sustained swimming, strenuous exercise, warming, or hypoxia. The level of demand at which such a mismatch may appear cannot be established from SMR data alone.

As SMR and MMR may follow different ontogenetic scaling trajectories, a GSA relationship observed under standard metabolic conditions cannot be assumed to apply equally to maximum metabolic demand or aerobic scope [47].

Table 2 should therefore be interpreted as a test of baseline metabolic scaling rather than as a direct test of maximal aerobic performance. AMR, MMR, or aerobic scope datasets measured under comparable thermal and experimental conditions would be required to evaluate whether gill surface area constrains oxygen supply during sustained or maximal activity [12,46]. The horn-shark study [52] was not incorporated into Table 2 because GSA showed an explicit ontogenetic breakpoint, whereas the reported resting and maximum-metabolic-rate exponents represented broader body-size ranges. Reducing these relationships to a single paired difference would obscure the developmental change in GSA scaling.

3.6. An Integrated Oxygen-Cascade Framework

The data presented in the previous sections can support a conceptual model of aerobic capacity in fish which views aerobic capacity as an emergent property of the oxygen transport cascade. If it is assumed that gill respiratory surface is the first entry point from which oxygen enters the transport pathway, it can be argued that its contribution to aerobic performance is contingent on the capacity of each subsequent step to sustain an equivalent flux. Following this first entry boundary, blood oxygen-carrying capacity and haemoglobin affinity set the amount of oxygen transported per unit blood volume; cardiac output governs the rate at which that oxygen is delivered to the tissues; capillary geometry and fibre architecture establish the diffusion pathway at the tissue level; mitochondrial phenotype determines the rate of terminal oxygen consumption coupled to ATP synthesis; and body form together with swimming ecology sets the overall demand that the cascade must meet (Figure 1, Table 3). The model predicts that gill area should be most strongly related to performance when branchial uptake is directly impaired, when oxygen availability is low, or when metabolic demand increases without compensatory changes downstream. It predicts weaker relationships when cardiovascular, haematological, or muscular traits compensate for gill scaling, or when ecological strategy reduces routine oxygen demand. This framing explains why gill area can be experimentally limiting in rainbow trout or diseased Atlantic salmon, yet insufficient as a universal predictor across taxa with different blood, heart, and muscle phenotypes.

Table 3. Integrated O_2 cascade model for interpreting gill area–performance relationships.

Oxygen Cascade Component	Primary Variables	Expected Effect on Aerobic Capacity	References
Gill respiratory surface	Gill area, secondary lamellae, diffusion distance, ILCM, lamellar perfusion	Defines potential oxygen uptake from water.	[7–9]
Blood oxygen transport	Haemoglobin concentration, haematocrit, erythrocyte traits, Hb-O_2 affinity, Bohr/Root effects	Determines oxygen transport per unit blood volume and unloading capacity.	[5]
Cardiac delivery	Heart mass, stroke volume, heart rate, cardiac output, myocardial oxidative capacity	Moves oxygen from gills to tissues; may compensate for size-related constraints.	[6,20]

Table 3. *Cont.*

Oxygen Cascade Component	Primary Variables	Expected Effect on Aerobic Capacity	References
Tissue capillarity and fibre geometry	Capillary density, capillaries per fibre, fibre diameter, diffusion distance	Controls final oxygen delivery to active fibres.	[10,39]
Mitochondrial phenotype	Mitochondrial volume density, cristae density, CS, COX, SDH, mitochondrial respiration	Determines terminal aerobic ATP production and oxygen use.	[25,41]
Body form and ecology	Caudal fin aspect ratio, body form, swimming mode, habitat, temperature range, hypoxia exposure	Sets oxygen demand and selection on the cascade.	[11]
Branchial Ventilation	Ventilation frequency, ventilatory stroke volume, ram ventilation, water flow	Delivers oxygenated water to the lamellae and may compensate for variation or reduction in anatomical GSA	[18,19]

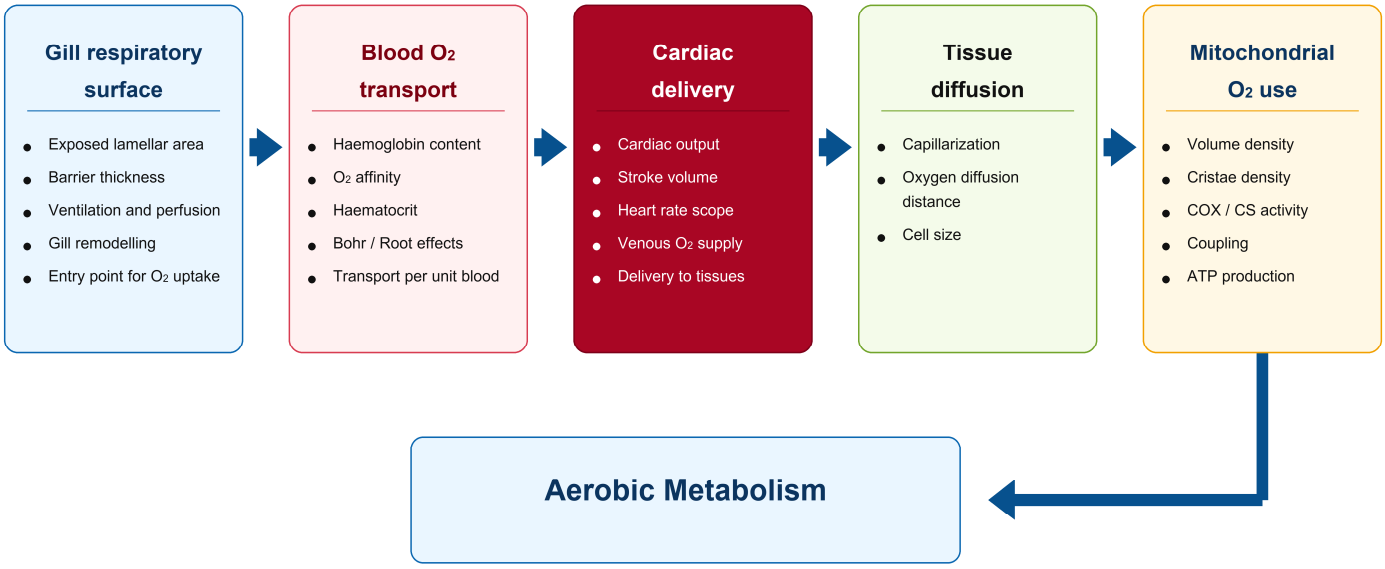

Figure 1. Conceptual oxygen-cascade model linking gill respiratory surface to aerobic metabolism in fishes. Gill respiratory surface provides the anatomical entry point for oxygen uptake, but realised oxygen flux depends on branchial ventilation and perfusion, blood oxygen transport, cardiac delivery, tissue diffusion, and mitochondrial oxygen use. Red skeletal muscle is shown as a focal example of the tissue-delivery stage because its capillary supply, fibre geometry, and oxidative phenotype are particularly important during sustained aerobic swimming; it is not intended to represent the exclusive terminal tissue of the cascade. Mitochondrial oxygen use occurs in all metabolically active tissues, and whole-animal SMR integrates oxygen consumption across multiple organs and tissues. Moreover, anatomical capillary density alone does not determine functional oxygen delivery, which also depends on perfusion, capillary topology, tissue geometry, and local metabolic demand [24].

4. Discussion

Across the ten paired SMR datasets, the direction and magnitude of $b_{GSA} - b_{SMR}$ varied among species and experimental conditions, with negative, near-zero, and positive differences all represented. The evidence presented above indicates that gill surface area is an important but conditional determinant of aerobic capacity in fishes. Experimental studies show that reductions in functional gill area can reduce maximal oxygen consumption and swimming performance, while reversible gill remodelling can increase exposed lamellar area under hypoxia or elevated oxygen demand.

Comparative studies further support the importance of gill surface area, while also showing that its explanatory power is incomplete when considered in isolation [5,10,11]. Gill area explains part of the interspecific variation in oxygen consumption and hypoxia tolerance, whereas routine metabolic demand, haemoglobin–oxygen affinity, and muscle

capillarity account for additional variation [5,10]. More broadly, cardiac delivery and tissue oxidative phenotype may further modify the relationship between branchial oxygen uptake and realised aerobic performance [6,28].

The arithmetic and inverse-variance-weighted summaries were close to zero, but these values are treated only as descriptive summaries because the datasets are heterogeneous but the data indicate the absence of a consistently negative directional pattern. Within the limits of the available datasets, this does not support a general decline in gill surface area relative to maintenance metabolic demand across the body-size ranges examined. This should not be interpreted as a complete test of GOLT across all metabolic states, because constraints may emerge during routine swimming, maximal activity, warming, hypoxia, or disease without being evident under standard metabolic conditions. This interpretation shifts the emphasis from a simple gill-limitation model to an integrated oxygen-cascade framework. Gill surface area may become strongly predictive of aerobic capacity when branchial uptake is experimentally reduced, when oxygen availability is low, when lamellar surface is remodelled, or when metabolic demand increases without equivalent downstream compensation. Conversely, its predictive value may be weakened when cardiovascular, haematological, or muscular traits compensate for branchial constraints. Large salmonids, for example, may partly offset size-related respiratory limitations through cardiac and haematological adjustments, while cyprinids may alter functional lamellar surface area through reversible gill remodelling.

Haemoglobinless icefishes represent a more extreme reorganisation of the oxygen transport pathway, one in which the absence of respiratory pigment is compensated through cardiac enlargement, elevated cardiac output, and structural adaptations that favour tissue-level diffusion.

At the level of skeletal muscle, capillary density, fibre diameter, and intracellular diffusion distance collectively govern whether oxygen arriving at the tissue can reach the mitochondria at a rate sufficient to sustain aerobic metabolism. The terminal step—oxygen consumption coupled to ATP synthesis—is then a function of mitochondrial volume density, cristae surface density, and the activity of oxidative enzymes. That gill surface area alone proves insufficient to predict aerobic swimming performance, hypoxia tolerance, or thermal sensitivity across species is, in large part, a consequence of this downstream variability; two species may present comparable gill area but may exhibit differences in their aerobic capacity, if for example they differ in muscle capillarization or qualitative and quantitative differences in their mitochondrial content.

Future analyses should test this framework using matched datasets in which gill surface area, SMR, AMR or MMR, aerobic scope, blood oxygen-carrying capacity, cardiac output, muscle capillarity, and mitochondrial or enzymatic traits are measured under comparable temperature and oxygen conditions. The bGSA-bSMR comparison presented here was based on published SMR scaling exponents and was used to examine whether the available datasets show a consistent size-related decline in GSA relative to baseline maintenance demand. Because metabolic and respiratory allometries may vary among life stages, ecological contexts, and experimental conditions rather than following fixed universal exponents [55,58], the present comparison should be regarded as a restricted, data-supported application of the oxygen-cascade framework. Its principal observation—the absence of a consistently negative GSA–SMR scaling difference—should be evaluated using broader, size-matched datasets that also include routine activity, AMR/MMR, aerobic scope, hypoxia exposure, and thermal challenge.

In the SMR datasets analysed here, the paired differences between gill surface area and SMR scaling were not consistently negative across the available datasets, although their direction and magnitude varied among species and conditions across the available

size ranges. This result should not be interpreted as excluding oxygen limitation under maximal activity, warming, hypoxia, disease or rapid growth. Rather, it supports an oxygen-cascade interpretation in which the predictive value of gill area depends on integration with blood oxygen transport, cardiac delivery, muscle diffusion capacity, and mitochondrial oxygen use.

5. Conclusions

The evidence reviewed supports a conditional rather than universal role of gill respiratory surface in the aerobic metabolism of fishes. Experimental reductions in functional gill area can impair oxygen uptake and swimming performance, whereas ventilatory compensation and reversible gill remodelling may preserve or increase realised branchial oxygen-transfer capacity. Across the ten paired SMR datasets examined, the differences between GSA and SMR scaling were negative, near zero, or positive, and therefore did not reveal a consistently negative size-related mismatch between gill surface area and baseline maintenance oxygen demand. This restricted result does not exclude branchial limitation during sustained swimming, maximal activity, warming, hypoxia, disease, or rapid growth. Gill area is therefore neither universally limiting nor physiologically unimportant. Its predictive value depends on metabolic state, ontogenetic stage, and integration with ventilation, blood oxygen transport, cardiac delivery, tissue diffusion, and mitochondrial oxygen use.

Funding: This research received no external funding.

Institutional Review Board Statement: Not applicable.

Data Availability Statement: No new data were created in this study.

Conflicts of Interest: The author declares no conflicts of interest.

References

1. Pauly, D. The Gill-Oxygen Limitation Theory (GOLT) and its critics. *Sci. Adv.* **2021**, *7*, eabc6050. [CrossRef] [PubMed]
2. Pauly, D.; Muller, J. Fick's Diffusion Laws and Scaling of the Gill Surface Area and Oxygen Uptake in Fish. *Fishes* **2025**, *10*, 233. [CrossRef]
3. Chabot, D.; Steffensen, J.F.; Farrell, A.P. The determination of standard metabolic rate in fishes. *J. Fish Biol.* **2016**, *88*, 81–121. [CrossRef] [PubMed]
4. Evans, D.H.; Piermarini, P.M.; Choe, K.P. The multifunctional fish gill: Dominant site of gas exchange, osmoregulation, acid-base regulation, and excretion of nitrogenous waste. *Physiol. Rev.* **2005**, *85*, 97–177. [CrossRef] [PubMed]
5. Mandic, M.; Todgham, A.E.; Richards, J.G. Mechanisms and evolution of hypoxia tolerance in fish. *Proc. R. Soc. B* **2009**, *276*, 735–744. [CrossRef] [PubMed]
6. Clark, T.D.; Farrell, A.P. Effects of body mass on physiological and anatomical parameters of mature salmon: Evidence against a universal heart rate scaling exponent. *J. Exp. Biol.* **2011**, *214*, 887–893. [CrossRef] [PubMed]
7. Duthie, G.G.; Hughes, G.M. The effects of reduced gill area and hyperoxia on the oxygen consumption and swimming speed of rainbow trout. *J. Exp. Biol.* **1987**, *127*, 349–354. [CrossRef]
8. Fu, S.-J.; Brauner, C.J.; Cao, Z.-D.; Richards, J.G.; Peng, J.-L.; Dhillon, R.; Wang, Y.-X. The effect of acclimation to hypoxia and sustained exercise on subsequent hypoxia tolerance and swimming performance in goldfish. *J. Exp. Biol.* **2011**, *214*, 2080–2088. [CrossRef] [PubMed]
9. Hvas, M.; Karlsbakk, E.; Maehle, S.; Wright, D.W.; Oppedal, F. The gill parasite *Paramoeba perurans* compromises aerobic scope, swimming capacity and ion balance in Atlantic salmon. *Conserv. Physiol.* **2017**, *5*, cox066. [CrossRef] [PubMed]
10. Crans, K.D.; Pranckevicius, N.A.; Scott, G.R.; Richards, J.G. Physiological tradeoffs may underlie the evolution of hypoxia tolerance and exercise performance in sunfish. *J. Exp. Biol.* **2015**, *218*, 3264–3275. [CrossRef] [PubMed]
11. Kuparinen, A.; Gielewski, D.; Hutchings, J.A. Gill area explains deviations from body size–metabolic rate relationship in teleost fishes. *J. Fish Biol.* **2022**, *101*, 308–311. [CrossRef] [PubMed]
12. Scheuffele, H.; Jutfelt, F.; Clark, T.D. Investigating the gill-oxygen limitation hypothesis in fishes: Intraspecific scaling relationships of metabolic rate and gill surface area. *Conserv. Physiol.* **2021**, *9*, coab040. [CrossRef] [PubMed]

13. Perry, S.F.; Fletcher, C.; Bailey, S.; Ting, J.; Bradshaw, J.; Tzaneva, V.; Gilmour, K.M. The interactive effects of exercise and gill remodeling in goldfish (*Carassius auratus*). *J. Comp. Physiol. B* **2012**, *182*, 935–945. [CrossRef] [PubMed]
14. Sollid, J.; Weber, R.E.; Nilsson, G.E. Temperature alters the respiratory surface area of crucian carp *Carassius carassius* and goldfish *Carassius auratus*. *J. Exp. Biol.* **2005**, *208*, 1109–1116. [CrossRef] [PubMed]
15. Sollid, J.; Nilsson, G.E. Plasticity of respiratory structures: Adaptive remodeling of fish gills induced by ambient oxygen and temperature. *Respir. Physiol. Neurobiol.* **2006**, *154*, 241–251. [CrossRef] [PubMed]
16. Nilsson, G.E. Gill remodeling in fish: A new fashion or an ancient secret? *J. Exp. Biol.* **2007**, *210*, 2403–2409. [CrossRef] [PubMed]
17. Mitrovic, D.; Perry, S.F. The effects of thermally induced gill remodeling on ionocyte distribution and branchial chloride fluxes in goldfish (*Carassius auratus*). *J. Exp. Biol.* **2009**, *212*, 843–852. [CrossRef] [PubMed]
18. Luo, Y.; Li, Q.; Zhu, X.; Zhou, J.; Shen, C.; Xia, D.; Djiba, P.K.; Xie, H.; Lv, X.; Jia, J.; et al. Ventilation frequency reveals the roles of exchange surface areas in metabolic scaling. *Physiol. Biochem. Zool.* **2020**, *93*, 13–22. [CrossRef] [PubMed]
19. Xiong, W.; Zhu, Y.; Zhu, X.; Li, Q.; Luo, Y. Effects of gill excision and food deprivation on metabolic scaling in the goldfish *Carassius auratus*. *J. Exp. Zool. A Ecol. Integr. Physiol.* **2020**, *333*, 194–200. [CrossRef] [PubMed]
20. Rodnick, K.J.; Williams, S.R. Effects of body size on biochemical characteristics of trabecular cardiac muscle and plasma of rainbow trout (*Oncorhynchus mykiss*). *Comp. Biochem. Physiol. A* **1999**, *122*, 407–413. [CrossRef]
21. Deitch, E.J.; Fletcher, G.L.; Petersen, L.H.; Costa, I.A.S.F.; Shears, M.A.; Driedzic, W.R.; Gamperl, A.K. Cardiorespiratory modifications, and limitations, in post-smolt growth hormone transgenic Atlantic salmon Salmo salar. *J. Exp. Biol.* **2006**, *209*, 1310–1325. [CrossRef] [PubMed]
22. Kuchenmuller, L.L.; Ekstrom, A.; Hoots, E.C.; Skeeles, M.R.; Sandblom, E.; Clark, T.D. Evidence for size-dependent cardiac oxygen supply in a fish. *J. Exp. Biol.* **2025**, *228*, jeb250857. [CrossRef] [PubMed]
23. Egginton, S.; Cordiner, S. Cold-induced angiogenesis in seasonally acclimatized rainbow trout (*Oncorhynchus mykiss*). *J. Exp. Biol.* **1997**, *200*, 2263–2268. [CrossRef] [PubMed]
24. Egginton, S. Anatomical adaptations for peripheral oxygen transport at high and low temperatures. *S. Afr. J. Zool.* **1998**, *33*, 119–128. [CrossRef]
25. O'Brien, K.M.; Skilbeck, C.; Sidell, B.D.; Egginton, S. Muscle fine structure may maintain the function of oxidative fibres in haemoglobinless Antarctic fishes. *J. Exp. Biol.* **2003**, *206*, 411–421. [CrossRef] [PubMed]
26. O'Brien, K.M. Mitochondrial biogenesis in cold-bodied fishes. *J. Exp. Biol.* **2011**, *214*, 275–285. [CrossRef] [PubMed]
27. Gatz, A.J., Jr. Speed, stamina, and muscles in fishes. *J. Fish. Res. Board Can.* **1973**, *30*, 325–328. [CrossRef]
28. Norin, T.; Malte, H. Intraspecific variation in aerobic metabolic rate of fish: Relations with organ size and enzyme activity in Brown Trout. *Physiol. Biochem. Zool.* **2012**, *85*, 645–656. [CrossRef] [PubMed]
29. Eliason, E.J.; Higgs, D.A.; Farrell, A.P. Postprandial gastrointestinal blood flow, oxygen consumption and heart rate in rainbow trout (*Oncorhynchus mykiss*). *Comp. Biochem. Physiol. A Mol. Integr. Physiol.* **2008**, *149*, 380–388. [CrossRef] [PubMed]
30. Glazier, D.S.; Borrelli, J.J.; Hoffman, C.L. Effects of fish predators on the mass-related energetics of a keystone freshwater crustacean. *Biology* **2020**, *9*, 40. [CrossRef] [PubMed]
31. Richards, J.G.; Mercado, A.J.; Clayton, C.A.; Heigenhauser, G.J.; Wood, C.M. Substrate utilization during graded aerobic exercise in rainbow trout. *J. Exp. Biol.* **2002**, *205*, 2067–2077. [CrossRef] [PubMed]
32. Hwang, P.P.; Lee, T.H.; Lin, L.Y. Ion regulation in fish gills: Recent progress in the cellular and molecular mechanisms. *Am. J. Physiol. Regul. Integr. Comp. Physiol.* **2011**, *301*, R28–R47. [CrossRef] [PubMed]
33. Guderley, H. Metabolic responses to low temperature in fish muscle. *Biol. Rev.* **2004**, *79*, 409–427. [CrossRef] [PubMed]
34. Guderley, H.; Lavoie, B.A.; Dubois, N. The interaction among age, thermal acclimation and growth rate in determining muscle metabolic capacities and tissue masses in the threespine stickleback, *Gasterosteus aculeatus*. *Fish Physiol. Biochem.* **1994**, *13*, 419–431. [CrossRef] [PubMed]
35. Nathanailides, C. Are changes in enzyme activities of fish muscle during cold acclimation significant? *Can. J. Fish. Aquat. Sci.* **1996**, *53*, 2333–2336. [CrossRef]
36. Nathanailides, C.; Stickland, N.C. Activity of cytochrome c oxidase and lactate dehydrogenase in muscle tissue of slow growing (lower modal group) and fast growing (upper modal group) Atlantic salmon. *J. Fish Biol.* **1996**, *48*, 549–551. [CrossRef]
37. Makri, V.; Giantsis, I.A.; Nathanailides, C.; Feidantsis, K.; Antonopoulou, E.; Theodorou, J.A.; Michaelidis, B. Seasonal energy investment and metabolic patterns in a farmed fish. *J. Therm. Biol.* **2024**, *123*, 103894. [CrossRef] [PubMed]
38. Johnston, I.A. Capillarisation, oxygen diffusion distances and mitochondrial content of carp muscles following acclimation to summer and winter temperatures. *Cell Tissue Res.* **1982**, *222*, 325–337. [CrossRef] [PubMed]
39. Young, S.; Egginton, S. Allometry of skeletal muscle fine structure allows maintenance of aerobic capacity during ontogenetic growth. *J. Exp. Biol.* **2009**, *212*, 3564–3575. [CrossRef] [PubMed]
40. Egginton, S.; Sidell, B.D. Thermal acclimation induces adaptive changes in subcellular structure of fish skeletal muscle. *Am. J. Physiol.* **1989**, *256*, R1–R9. [CrossRef] [PubMed]

41. St-Pierre, J.; Charest, P.-M.; Guderley, H. Relative contribution of quantitative and qualitative changes in mitochondria to metabolic compensation during seasonal acclimatisation of rainbow trout *Oncorhynchus mykiss*. *J. Exp. Biol.* **1998**, *201*, 2961–2970. [CrossRef]
42. Verberk, W.C.E.P.; Atkinson, D.; Hoefnagel, K.N.; Hirst, A.G.; Horne, C.R.; Siepel, H. Shrinking body sizes in response to warming: Explanations for the temperature-size rule with special emphasis on the role of oxygen. *Biol. Rev.* **2021**, *96*, 247–268. [CrossRef] [PubMed]
43. Verberk, W.C.E.P.; Sandker, J.F.; van de Pol, I.L.E.; Urbina, M.A.; Wilson, R.W.; McKenzie, D.J.; Leiva, F.P. Body mass and cell size shape the tolerance of fishes to low oxygen in a temperature-dependent manner. *Glob. Change Biol.* **2022**, *28*, 5695–5707. [CrossRef] [PubMed]
44. Earhart, M.L.; Blanchard, T.S.; Harman, A.A.; Schulte, P.M. Hypoxia and high temperature as interacting stressors: Will plasticity promote resilience of fishes in a changing world? *Biol. Bull.* **2022**, *243*, 149–170. [CrossRef] [PubMed]
45. Leonard, J.N.; Skov, P.V. Capacity for thermal adaptation in Nile tilapia (*Oreochromis niloticus*): Effects on oxygen uptake and ventilation. *J. Therm. Biol.* **2022**, *105*, 103206. [CrossRef] [PubMed]
46. Clark, T.D.; Sandblom, E.; Jutfelt, F. Aerobic scope measurements of fishes in an era of climate change: Respirometry, relevance and recommendations. *J. Exp. Biol.* **2013**, *216*, 2771–2782. [CrossRef] [PubMed]
47. Clark, T.D.; Sandblom, E.; Jutfelt, F. Response to Farrell and to Portner and Giomi. *J. Exp. Biol.* **2013**, *216*, 4495–4497. [CrossRef] [PubMed]
48. Portner, H.O.; Giomi, F. Nothing in experimental biology makes sense except in the light of ecology and evolution. *J. Exp. Biol.* **2013**, *216*, 4494–4495. [CrossRef] [PubMed]
49. Oikawa, S.; Itazawa, Y. Gill and body surface areas of the carp in relation to body mass, with special reference to the metabolism-size relationship. *J. Exp. Biol.* **1985**, *117*, 1–14. [CrossRef]
50. Rombough, P.J.; Moroz, B.M. The scaling and potential importance of cutaneous and branchial surfaces in respiratory gas exchange in larval and juvenile walleye Stizostedion vitreum. *J. Exp. Biol.* **1997**, *200*, 2459–2468. [CrossRef] [PubMed]
51. Kim, D.I. Ontogeny of the respiratory area in relation to body mass with reference to resting metabolism in the Japanese flounder, *Paralichthys olivaceus* (Temminck & Schlegel, 1846). *Fishes* **2022**, *7*, 39. [CrossRef]
52. Prinzing, T.S.; Bigman, J.S.; Skelton, Z.R.; Dulvy, N.K.; Wegner, N.C. The allometric scaling of oxygen supply and demand in the California horn shark, *Heterodontus francisci*. *J. Exp. Biol.* **2023**, *226*, jeb246054. [CrossRef] [PubMed]
53. Kim, D.I. Ontogenetic phase shifts in metabolism and intraspecific scaling in a non-teleost fish, the Sterlet Sturgeon (*Acipenser ruthenus*). *Hydrobiology* **2025**, *4*, 24. [CrossRef]
54. Killen, S.S.; Costa, I.; Brown, J.A.; Gamperl, A.K. Little left in the tank: Metabolic scaling in marine teleosts and its implications for aerobic scope. *Proc. R. Soc. Lond. B Biol. Sci.* **2007**, *274*, 431–438.
55. Glazier, D.S. The 'fire of life cycles': Age-specific metabolic scaling within and among species. *J. Comp. Physiol. B* **2026**, *Online ahead of print*. [CrossRef] [PubMed]
56. Rosenfeld, J.S.; Van Leeuwen, T.E.; Richards, J.G.; Allen, D. Relationship between growth and standard metabolic rate: Measurement artefacts and implications for habitat use and life-history adaptation in salmonids. *J. Anim. Ecol.* **2015**, *84*, 4–20. [CrossRef] [PubMed]
57. Allen, D.; Rosenfeld, J.; Richards, J.G. Physiological basis of metabolic trade-offs between growth and performance among different strains of rainbow trout. *Can. J. Fish. Aquat. Sci.* **2016**, *73*, 1493–1506. [CrossRef]
58. Glazier, D.S. Scaling species interactions: Implications for community ecology and biological scaling theory. *Acad. Biol.* **2023**, *1*, 1–20. [CrossRef]